

# International Journal of Bio-Inorganic Hybrid Nanomaterials

## Synthesis of Iron Oxide Nanoparticles using Borohydride Reduction

Majid Farahmandjou<sup>1\*</sup>, Farzaneh Soflaee<sup>2</sup>

<sup>1</sup> Assistant Professor, Department of Physics, Varamin Pishva Branch, Islamis Azad University, Varamin, Iran

<sup>2</sup> M.Sc., Department of Physics, Varamin Pishva Branch, Islamis Azad University, Varamin, Iran

Received: 9 July 2014; Accepted: 13 September 2014

### ABSTRACT

Iron oxide ( $\text{Fe}_2\text{O}_3$ ) nanoparticles were synthesized by a simple approach using sodium borohydride ( $\text{NaBH}_4$ ) and Iron chloride hexahydrate ( $\text{FeCl}_3 \cdot 6\text{H}_2\text{O}$ ). Their physicochemical properties were characterized by high resolution transmission electron microscopy (HRTEM), scanning electron microscopy (SEM), X-ray diffraction (XRD) and electron dispersive spectroscopy (EDS). XRD pattern showed that the iron oxide nanoparticles exhibited rhombohedral structure and  $\gamma\text{-Fe}_2\text{O}_3$  (maghemite) to  $\alpha\text{-Fe}_2\text{O}_3$  (hematite) structural phase transition in nanocrystals. The particle size of  $\alpha\text{-Fe}_2\text{O}_3$  was around 28 nm in diameter as estimated by XRD technique. The surface morphological studies from SEM depicted spherical particles with formation of clusters by increasing annealing temperature. The EDS spectrum showed peaks of iron and oxygen free of impurity.

**Keyword:** Iron oxide nanoparticles; Sodium borohydride reduction; Synthesis; Hematite; Crystal structure; Morphological properties.

## 1. INTRODUCTION

Magnetic nanoparticles have unique physiochemical and optical properties due to surface and finite-size effects. These promising magnetic nanoparticles have been widely used as microwave radiation absorbers [1, 2], spin-based devices [3], cathode materials of lithium battery [4], ferrofluids [5, 6], drug-targeting and cell separation carriers [7]. Several types of iron oxides have been studied by researchers such  $\text{Fe}_3\text{O}_4$  (magnetite),  $\alpha\text{-Fe}_2\text{O}_3$  (hematite),  $\gamma\text{-Fe}_2\text{O}_3$  (maghemite),

$\text{FeO}$  (wustite),  $\epsilon\text{-Fe}_2\text{O}_3$  and  $\beta\text{-Fe}_2\text{O}_3$  [8], among which magnetite and maghemite is the very important in magnetic application. Magnetic iron oxide nanoparticles have a large surface-to-volume ratio and therefore possess high surface energies. There are several methods to preparation of the iron oxid nanoparticles such as co-precipitation, thermal decomposition, hydrothermal synthesis, sol-gel synthesis, microemulsion, sonochemical synthesis, and sonochemical synthetic route

(\* Corresponding Author - e-mail: farahmandjou@iauvaramin.ac.ir

[9, 13]. In the following, we focus mainly on chemical reduction of the iron oxide nanoparticles using Iron chloride hexahydrate ( $\text{FeCl}_3 \cdot 6\text{H}_2\text{O}$ ). Morphological properties are discussed by XRD, TEM, SEM and EDS analyses.

## 2. EXPERIMENTAL DETAIL

Iron oxide nanoparticles were synthesized by a new borohydride reduction approach according to the following manner. Firstly, 15 g of  $\text{FeCl}_3 \cdot 6\text{H}_2\text{O}$  was dissolved in 150 mL pure water with stirring and then 2 g  $\text{NaBH}_4$  was added to the solution and temperature was increased to  $80^\circ\text{C}$ . The color of solution changed from bright to dark. The pH for the solvent was maintained during the synthesis around 1.

The product was synthesized for 2 hours at the mentioned temperature, cooled to room temperature and finally calcined at  $500^\circ\text{C}$  for 4 hours. All analyses were done for samples without any washing and purification. The specification of the size, structure and surface morphological properties of the as-synthesis and annealed  $\text{Fe}_2\text{O}_3$  nanoparticles were carried out. X-ray diffractometer (XRD) was used to identify the crystalline phase and to estimate the crystalline size. The XRD pattern were recorded with  $2\theta$  in the range of  $4-85^\circ$  with type X-Pert Pro MPD,  $\text{Cu-K}_\alpha$ ;  $\lambda = 1.54 \text{ \AA}$ . The morphology was characterized by field emission scanning electron

microscopy (SEM) with type KYKY-EM3200, 25 kV and transmission electron microscopy (TEM) with type Zeiss EM-900, 80 kV. The Fe and O elemental analysis of the samples was performed by energy dispersive spectroscopy (EDS) type VEGA, 15 kV. All the measurements were carried out at room temperature.

## 3. RESULTS AND DISCUSSION

X-ray diffraction (XRD) at 40Kv was used to identify crystalline phases and to estimate the crystalline sizes. Figure 1 shows the X-ray diffraction patterns of the powder before and after heat treatment. Figure 1(a) shows the XRD pattern of Iron oxide before annealing. A  $\gamma \rightarrow \alpha\text{-Fe}_2\text{O}_3$  phase transformation took place during calcination between 300 and  $400^\circ\text{C}$  [9]. Figure 1(b) shows the XRD pattern of Iron oxide after annealing. An abrupt increase in the amount of a phase occurred when the calcinations temperature rose above  $500^\circ\text{C}$ .  $\alpha\text{-Fe}_2\text{O}_3$  was the only phase present for the powder calcined above  $500^\circ\text{C}$  [12]. The exhibited picks correspond to the (012), (104), (110), (113), (024), (116), (018), (214) and (300) of a rhombohedral (hexagonal) structure of  $\alpha\text{-Fe}_2\text{O}_3$  is identified using the standard data. The mean size of the ordered  $\text{Fe}_2\text{O}_3$  nanoparticles has been estimated from full width at half maximum (FWHM) and Debye-Scherrer formula according to equation the fol-

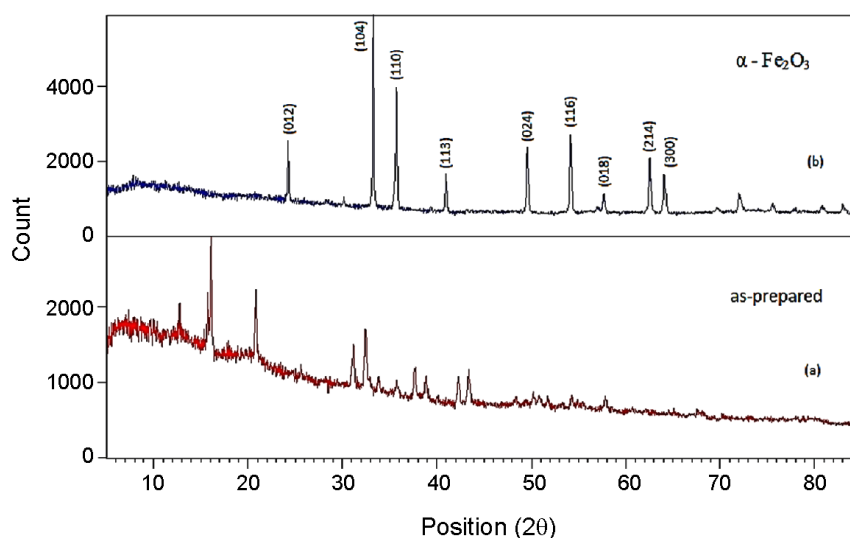


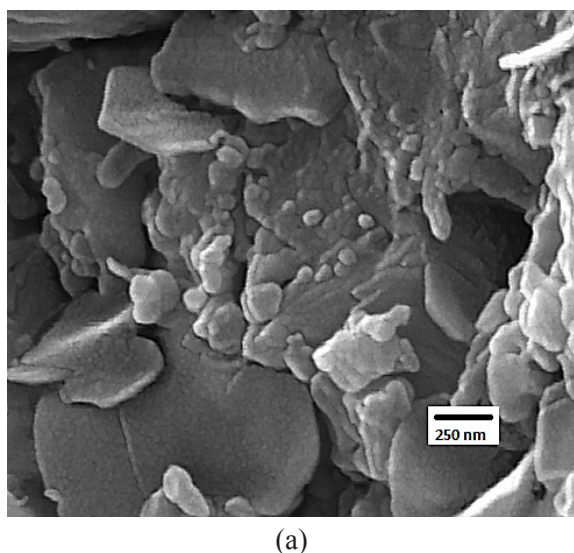
Figure 1: XRD pattern of iron oxide nanoparticles.

lowing:

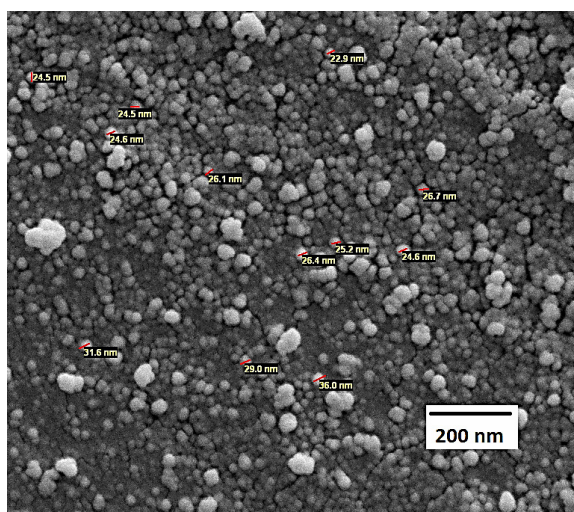
$$D = \frac{0.89\lambda}{B \cos \theta} \quad (1)$$

where, 0.89 is the shape factor,  $\lambda$  is the X-ray wavelength, B is the line broadening at half the maximum intensity (FWHM) in radians, and  $\theta$  is the Bragg angle. The mean size of as-prepared  $\alpha$ -Fe<sub>2</sub>O<sub>3</sub> nanoparticles was around 28 nm from this Debye-Scherrer equation. The lattice constant so obtained for alpha Fe<sub>2</sub>O<sub>3</sub> nanoparticles were a= b= 5.0352 Å and c= 13.7480 Å.

The scanning electron microscope (SEM) was



(a)



(b)

**Figure 2:** SEM images of the Fe<sub>2</sub>O<sub>3</sub> nanoparticles (a) as-prepared (b) annealed at 500°C.

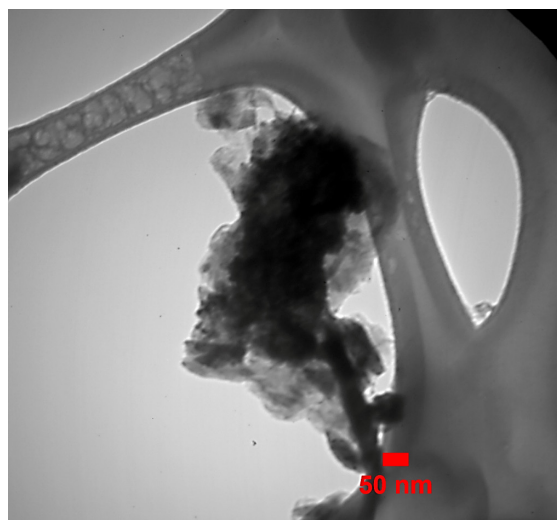


**Figure 3:** TEM image of as-prepared Fe<sub>2</sub>O<sub>3</sub> nanoparticles.

used for the morphological study of nanoparticles of Fe<sub>2</sub>O<sub>3</sub> samples. These analyses show that high homogeneity emerged in the samples surface by increasing annealing temperature. With increasing temperature the morphology of the particles changes to the spherical shape and nanopowders were less agglomerate. Figure 2(a) shows the SEM image of the as-prepared Fe<sub>2</sub>O<sub>3</sub> nanoparticles prepared by chemical reduction method. In this Figure, the particles prepared with formation of clusters. Figure 2(b) shows the SEM image of the annealed Fe<sub>2</sub>O<sub>3</sub> nanoparticles at 500°C for 4 hours. The Fe<sub>2</sub>O<sub>3</sub> nanoparticles formed were not aggregated. The spherical shaped particles with clumped distributions are visible through the SEM analysis. The SEM observation, the size of annealed nanocrystals is in the range of 24-32 nm in diameter.

The transmission electron microscopic (TEM) analysis was carried out to confirm the actual size of the particles, their growth pattern and the distribution of the crystallites. Figure 3 shows the as-synthesized TEM image of spherical Fe<sub>2</sub>O<sub>3</sub> nanoparticles prepared by chemical reduction route. It can be seen that nanoparticles were prepared with less aggregation.

Energy dispersive spectroscopy (EDS) of Fe<sub>2</sub>O<sub>3</sub> prepared by wet synthesis is shown in Figure 4 which confirms the existence of Fe and O with weight percent. EDS was used to analyze the chemical composition of a material under SEM. EDS shows peaks of iron and oxygen with fewer chlorine and sodium element.

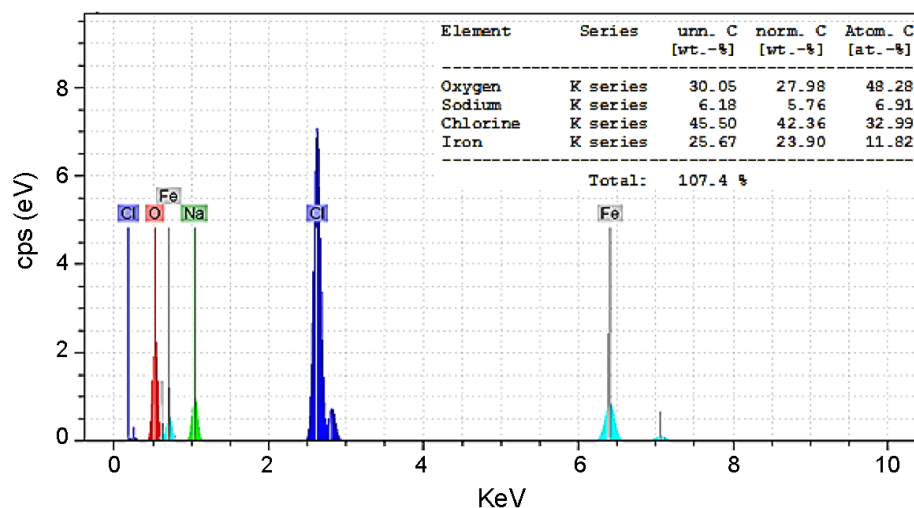


Figure 4: EDS spectra of the as-synthesized  $\text{Fe}_2\text{O}_3$  prepared by wet synthesis.

#### 4. CONCLUSIONS

The  $\alpha\text{-Fe}_2\text{O}_3$  nanoparticles have been prepared using chemical reduction of iron chloride hexa hydrate and sodium borohydride. XRD spectrum shows rhombohedral (hexagonal) structure of  $\alpha\text{-Fe}_2\text{O}_3$ . From SEM images, it is clear that with increasing temperature the morphology of the particles changes to the spherical shape and nanopowders were less agglomerate. TEM image exhibits that the as-synthesized TEM image of spherical  $\text{Fe}_2\text{O}_3$  nanoparticles prepared by chemical reduction route with a diameter in the range of 24-32 nm with less aggregation. EDS shows only peaks of iron and oxygen and indicates the absence of impurities in prepared  $\text{Fe}_2\text{O}_3$ .

#### ACKNOWLEDGMENT

The authors are thankful for the financial support of Varamin Pishva Branch at Islamic Azad University for analysis and the discussions on the results.

#### REFERENCES

- Kirschvink J.L., *Bioelectromagnetics*, **17** (1996), 187.
- Kim D.K., Amin M.S., Elborai S., Lee S.H., Koseoglu Y., Zahn M. and Muhammed M., *J. Appl. Phys.*, **97** (2005), 10J510.
- Wang S., Yue F.J., Wu D., Zhang F.M., Zhong W. and Du Y.W., *Appl. Phys. Lett.*, **94** (2009), 012507.
- Ito S., Nakaoka K., Kawamura M., Ui K., Fujimoto K. and Koura N., *J. Power Sources.*, **146** (2005), 319.
- Nair S.S., Thomas J., Suchand Sandeep C.S., Anantharaman M.R. and Philip R., *Appl. Phys. Lett.*, **92** (2008), 171908.
- Wang X.F. and Shi L.Q., *Chin. Phys. B*, **19** (2010), 107502.
- Chen H.M., Deng C.H. and Zhang X.M., *Angew. Chem. Int. Ed.*, **49** (2010), 607.
- R.M. Cornell, U. Schwertmann, 2003. *The Iron Oxides: Structures, Properties, Reactions, Occurrences and Uses*, Wiley-VCH, Weinheim.
- Cabrera L., Gutierrez S., Menendezb N., Morales M.P., Herrasti P., *Electrochim. Acta*, **53** (2008), 3436.
- Pascal C., Pascal J.L., Favier F., Moubtassim M.L.E., Payen, *C. Chem. Mater.*, **11** (1999), 141.
- Bomati-Miguel O., Mazeina L., Navrotsky A., Veintemillas-Verdaguer S., *Chem. Mater.*, **20** (2008), 591.
- Bharde A.A., Parikh R.Y., Baidakova M., Jouen S., Hannoyer B., Enoki T. et al., *Langmuir*, **24** (2008), 5787.
- Roh Y., Vali H., Phelps T.J., Moon J.W., *J. Nanosci. Nanotechnol.*, **11** (2006), 3517.